



Controllable bulk solvent-free melt ring-opening polymerization (ROP) of L-lactide catalyzed by Ni(II) and Ni(II)–Ln(III) complexes based on the Salen-type Schiff-base ligand

Wen-Juan Jin^a, Li-Qin Ding^{a,b}, Zeng Chu^a, Lei-Lei Chen^a, Xing-Qiang Lü^{a,c,*},
Xiao-Yan Zheng^a, Ji-Rong Song^a, Dai-Di Fan^a

^a Shaanxi Key Laboratory of Degradable Medical Material, Shaanxi Key Laboratory of Physico-inorganic Chemistry, Northwest University, Xi'an 710069, Shaanxi, China

^b School of Chemistry & Chemical Engineering, Xi'an Shiyou University, Xi'an 710065, Shaanxi, China

^c State Key Laboratory of Structure Chemistry, Fujian Institute of Research on the Structure of Matter, Chinese Academy of Sciences, Fuzhou 350002, Fujian, China

ARTICLE INFO

Article history:

Received 31 May 2010

Received in revised form

22 November 2010

Accepted 10 January 2011

Available online 25 January 2011

Keywords:

Salen-type Schiff base transition metal or mixed metal complex

Bulk solvent-free melt ring-opening polymerization

L-Lactide

ABSTRACT

A monometallic (Ni²⁺, **1**) and a series of bimetallic (Ni²⁺–Ln³⁺, Ln = Ce (**2**); Ln = Nd (**3**); Ln = Sm (**4**); Ln = Eu (**5**); Ln = Tb (**6**); Ln = Ho (**7**); Ln = Tm (**8**)) complexes based on the Salen-type Schiff-base ligand **H₂L** (**H₂L** = N,N'-bis(3-methoxysalicylidene)ethylene-1,2-diamine) were synthesized and characterized by EA, FT-IR, ESI-MS and X-ray crystallography. The catalysis results showed that the two kinds of complexes with different active species, could efficiently catalyze the bulk solvent-free melt ring-opening polymerization (ROP) of L-lactide with moderate molecular weights and narrow molecular weight distributions. Especially for the series of bimetallic complexes **2–8**, the involvement of rare ions effectively passivated the catalytic behaviors on the ROP of L-lactide, while was in favor of the increase of polymeric molecular weights (*M_w* or *M_n*) and the polymerization controllability, and the type of rare ions was important and influential factor contributing to the catalytic behaviors.

© 2011 Elsevier B.V. All rights reserved.

1. Introduction

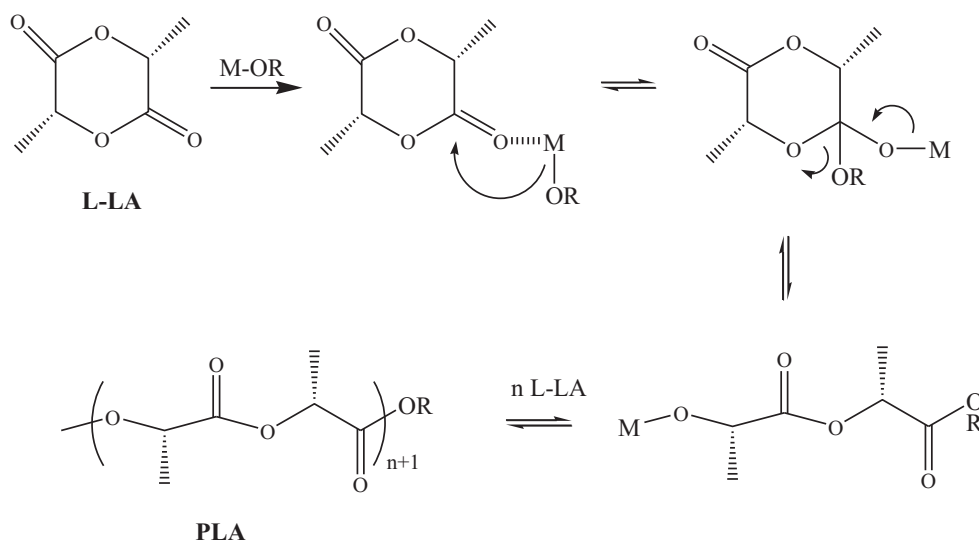
Poly(lactide) (PLA) polymers, as one of the biodegradable, biocompatible polyesters for wide-ranging use in medicine or pharmaceutical related applications [1], are mostly synthesized by the ring-opening polymerization (ROP) of lactide from diverse catalysts [2], both in solution polymerization and in bulk solvent-free melt polymerization. In spite of the well-established achievements in solution polymerization [3], commercially, the ROP of lactide is most commonly carried out with the bulk solvent-free melt polymerization [4], which exhibits advantages over solution polymerization: (i) no solvent is required; (ii) it is less vulnerable to impurity levels and unwanted side reactions; (iii) it is often useful for the large-scale production of PLAs [5]. From the viewpoint of needed catalysts with the bulk solvent-free melt polymerization, two kinds of typically molecular catalysts have been reported:

one is the metal complexes containing the characteristic initiators (alkoxide, amide or carboxylate), and the mechanism of the ROP of lactide is the same as that in solution polymerization, and generally recognized to proceed via the reaction pathway shown in Scheme 1, involving the attack of a characteristic group on the ketonic group of a coordinated lactide molecule [6]; the other is metal complexes lacking those normal initiators, while the excellent control of the polymerization could be well achieved from the molecular design of diverse catalysts and the selectivity of reaction conditions [7]. In spite of the limited knowledge on the possible polymerization mechanism [8], the coordination geometry and Lewis acidity of active species are probably responsible for metal-mediated ROP of lactide. Although these impressive recent developments are achieved, there has been an intense search for new generation catalysts for the bulk solvent-free melt ROP of lactide.

Compared to the homogeneous or heterogeneous catalysis of metal complexes based on Salen-type Schiff-base ligands in various chemical reactions [9], efforts of their use for the ring-opening polymerization of lactide are relatively limited [10]. Although many transition metal complexes [11] of Salen-type chiral or achiral Schiff-base ligands are well known to be efficient catalysts for the ring-opening polymerization of L-lactide, they are

* Corresponding author at: Shaanxi Key Laboratory of Degradable Medical Material, Shaanxi Key Laboratory of Physico-inorganic Chemistry, Northwest University, Taibai North Road 229, Xi'an 710069, Shaanxi, China. Tel.: +86 29 88302312; fax: +86 29 88302312.

E-mail address: lvxq@nwu.edu.cn (X.-Q. Lü).



Scheme 1. Schematic representation of the ROP process of L-lactide initiated by the M-OR complex.

just limited in the solution polymerization, and to the best of our knowledge, few report of their use for the bulk polymerization of L-lactide has been documented [12], especially there has no report on the mixed-metal (d-f) Salen-type Schiff-base complexes using as the catalysts for the ring-opening polymerization of L-lactide. Herein, we describe the syntheses, structures and the bulk solvent-free melt ROP of L-lactide of a monometallic (Ni^{2+} , **1**) and a series of bimetallic (Ni^{2+} - Ln^{3+} , $\text{Ln} = \text{Ce}$, **2**; $\text{Ln} = \text{Nd}$, **3**; $\text{Ln} = \text{Sm}$, **4**; $\text{Ln} = \text{Eu}$, **5**; $\text{Ln} = \text{Tb}$, **6**; $\text{Ln} = \text{Ho}$, **7**; $\text{Ln} = \text{Tm}$, **8**) complexes based on the Salen-type Schiff-base ligand H_2L ($\text{H}_2\text{L} = \text{N,N}'\text{-bis}(3\text{-methoxysalicylidene})\text{ethylene}$).

2. Experimental

All chemicals of reagent grade were commercially available and used without further purification. Element analyses were performed on a PerkinElmer 240C element analyzer. Infrared spectra were recorded on a Bruker EQUINOX55 FT-IR spectrophotometer in the region $4000\text{--}400\text{ cm}^{-1}$ in KBr pellets. ESI-MS was performed on a Finnigan LCQ^{DECA}XP HPLC-MSⁿ mass spectrometer with a mass to charge (m/z) range of 2000 using a standard electrospray ion source and toluene as solvent. ^1H NMR spectra were measured on a Varian Unity INOVA 400NB instrument using CDCl_3 as solvent and TMS as internal standard at room temperature. Electronic absorption spectra in the UV-visible region were recorded with a Hewlett Packard 8453 UV/Vis spectrophotometer. Thermogravimetric analyses were carried out on a NETZSCH TG 209 Instrument under flowing nitrogen by heating the samples from 25 to 600°C . MALDI-TOF MS analysis was carried out on a commercial Reflux III MALDI-TOF mass spectrometer (Bruker Co., Germany) equipped with delayed extraction technology. Ions formed by a pulsed UV laser beam with 3 nm pulse (nitrogen laser, $\lambda = 337\text{ nm}$) were accelerated through 20 kV and detection voltage was set at 1.60 kV. The laser was adjusted by the experiments slightly above the threshold, and the mass spectra were obtained from the results of 35 laser shots in positive mode.

2.1. Syntheses of the Salen-type Schiff-base ligand H_2L

The ligand H_2L was synthesized by the typical procedure [13] by condensation of *o*-vanillin (6.3 g, 40 mmol) and 1,2-diaminoethane (1.4 ml, 20 mmol) in absolute EtOH under reflux for about 5 h. After cooling to room temperature, the insoluble precipitate was filtered

and was re-crystallized using absolute EtOH to give the yellow polycrystalline solid. Yield: 5.0 g, 76%. Calc. for $\text{C}_{18}\text{H}_{20}\text{N}_2\text{O}_4$: C 65.84, H 6.14, N 8.53%; Found: C, 65.58, H, 6.06, N, 8.63%; IR (KBr, cm^{-1}): 3444 (b), 3001 (w), 2930 (w), 2840 (w), 1632 (s), 1468 (s), 1410 (m), 1249 (s), 1080 (m), 958 (m), 736 (m), 695 (w), 642 (w), 564 (w), 525 (w). ^1H NMR (400 MHz, CDCl_3): δ , 13.52 (s, 2H, -OH), 8.55 (s, 2H, -CH=N), 6.98 (m, 4H, -Ph), 6.75 (t, 2H, Ph), 3.91 (s, 4H, -CH₂), 3.74 (s, 6H, -MeO).

2.2. Synthesis of $[\text{NiL}](\mathbf{1})$

To a stirred solution of H_2L (0.164 g, 0.5 mmol) in absolute CH_2Cl_2 (5 ml), $\text{Ni}(\text{OAc})_2 \cdot 4\text{H}_2\text{O}$ (0.125 g, 0.5 mmol) was added and heated under reflux for 5 h. The mixture was allowed to cool to room temperature and filtered. The resultant clear brown solution was left to stand at room temperature for several days to give green polycrystalline product of **1** in 70% yield. Calc. for $\text{C}_{18}\text{H}_{18}\text{N}_2\text{O}_4\text{Ni}$: C, 56.15; H, 4.71; N, 7.28%; found: C, 56.38; H, 4.66; N, 7.35%. IR (KBr, cm^{-1}): 3291 (w), 2923 (w), 2828 (w), 1646 (s), 1603 (w), 1444 (vs), 1240 (m), 1215 (s), 728 (m), 697 (w), 636 (w), 582 (w), 531 (w), 463 (w). ^1H NMR (400 MHz, CDCl_3): δ , 8.51 (s, 2H, -CH=N), 7.05 (m, 4H, -Ph), 6.55 (t, 2H, Ph), 3.80 (s, 4H, -H₂), 3.74 (s, 6H, -MeO). ESI-MS (m/z): 386.04 $[\text{M}-\text{H}]^+$.

2.3. Syntheses of $[\text{Ni}(\text{L})\text{Ln}(\text{NO}_3)_3]$ ($\text{Ln} = \text{Ce}$, **2**; $\text{Ln} = \text{Nd}$, **3**; $\text{Ln} = \text{Sm}$, **4**; $\text{Ln} = \text{Eu}$, **5**; $\text{Ln} = \text{Tb}$, **6**; $\text{Ln} = \text{Ho}$, **7**; $\text{Ln} = \text{Tm}$, **8**)

To a solution of **1** (0.116 g, 0.3 mmol) in absolute EtOH (4 ml), a solution of $\text{Ln}(\text{NO}_3)_3 \cdot 6\text{H}_2\text{O}$ (0.3 mmol, $\text{Ln} = \text{Ce}$, 0.127 g; $\text{Ln} = \text{Nd}$, 0.132 g; $\text{Ln} = \text{Sm}$, 0.134 g; $\text{Ln} = \text{Eu}$, 0.134 g; $\text{Ln} = \text{Tb}$, 0.136 g; $\text{Ln} = \text{Ho}$, 0.138 g; $\text{Ln} = \text{Tm}$, 0.139 g) in absolute EtOH (5 ml) was added, respectively, and the mixture was refluxed for 3 h. Then 1 ml absolute DMF was added to give a respective clear brown solution. Diethyl ether was allowed to diffuse slowly into this solution at room temperature and deep red polycrystalline product of **2–8** was obtained in a few weeks, respectively. For **2**: Yield: 0.137 g (64%). Calc. for $\text{C}_{18}\text{H}_{18}\text{N}_5\text{O}_{13}\text{NiCe}$: C, 30.40; H, 2.55; N, 9.85%; found: C, 29.97; H, 2.66; N, 9.75%. IR (KBr, cm^{-1}): 3428 (w), 2953 (w), 1628 (s), 1559 (w), 1470 (vs), 1356 (w), 1296 (s), 1238 (m), 1170 (w), 1075 (w), 1052 (w), 1030 (w), 963 (w), 940 (w), 858 (w), 814 (w), 786 (w), 742 (m), 687 (w), 622 (w), 584 (w), 528 (w), 494 (w), 474 (w), 444 (w). ESI-MS (m/z): 649.17 $[\text{M}-\text{NO}_3]^+$. For **3**: Yield: 0.148 g (67%). Calc. for $\text{C}_{18}\text{H}_{18}\text{N}_5\text{O}_{13}\text{NiNd}$: C, 30.22; H, 2.54; N, 9.79%; found: C,

Table 1
Summary of crystallographic data and structure refinements for complexes **4**-CH₃COCH₃, **5**-CH₃COCH₃ and **6**-CH₃COCH₃.

Compound	4 -CH ₃ COCH ₃	5 -CH ₃ COCH ₃	6 -CH ₃ COCH ₃
Empirical formula	C ₂₁ H ₂₄ NiN ₅ O ₁₄ Sm	C ₂₁ H ₂₄ NiN ₅ O ₁₄ Eu	C ₂₁ H ₂₄ NiN ₅ O ₁₄ Tb
Formula weight	779.51	781.12	788.08
Crystal system	Monoclinic	Monoclinic	Monoclinic
Space group	Cc	Cc	Cc
<i>a</i> (Å)	11.276(2)	11.332(3)	11.308(2)
<i>b</i> (Å)	26.738(5)	26.905(8)	26.879(3)
<i>c</i> (Å)	9.177(2)	9.174(3)	9.187(1)
α (°)	90	90	90
β (°)	90	94.125(4)	94.295(1)
γ (°)	90	90	90
<i>V</i> (Å ³)	90	2798.8(15)	2784.6(5)
<i>Z</i>	4	4	4
ρ (g cm ⁻³)	1.876	1.860	1.880
<i>T</i> (K)	293(2)	296(2)	296(2)
Crystal size (mm ³)	0.33 × 0.26 × 0.23	0.38 × 0.26 × 0.25	0.33 × 0.26 × 0.23
μ (mm ⁻¹)	2.867	2.979	3.272
<i>F</i> (000)	1548	1552	1560
Data/restraints/parameters	3525/2/380	3776/2/379	4273/2/379
Quality-of-fit indicator	0.827	1.037	1.052
No. unique reflections	3525	3776	4273
No. observed reflections	7443	7354	6894
$[I > 2\sigma(I)]$			
<i>R</i>	0.0520	0.0417	0.0413
<i>wR</i>	0.1147	0.1123	0.1153

29.94; H, 2.67; N, 9.76%. IR (KBr, cm⁻¹): 3420 (w), 2952 (w), 1628 (s), 1561 (w), 1497 (m), 1466 (vs), 1352 (m), 1293 (s), 1235 (m), 1170 (m), 1077 (w), 1053 (w), 1028 (m), 963 (w), 856 (w), 814 (w), 785 (w), 739 (m), 672 (w), 631 (w), 584 (w), 528 (w), 492 (w), 471 (w), 441 (w). ESI-MS (*m/z*): 653.29 [M-NO₃]⁺. For **4**: Yield: 0.147 g (68%). Calc. for C₁₈H₁₈N₅O₁₃NiSm: C, 29.97; H, 2.51; N, 9.71%; found: C, 29.92; H, 2.72; N, 9.66%. IR (KBr, cm⁻¹): 3424 (w), 2987 (w), 2847 (w), 1630 (s), 1561 (w), 1498 (m), 1466 (vs), 1316 (w), 1276 (s), 1235 (m), 1166 (m), 1109 (w), 1080 (m), 1027 (w), 989 (w), 956 (w), 861 (w), 811 (w), 784 (w), 739 (m), 685 (w), 625 (w), 582 (w), 495 (w), 437 (w). ESI-MS (*m/z*): 659.41 [M-NO₃]⁺. For **5**: Yield: 0.132 g (61%). Calc. for C₁₈H₁₈N₅O₁₃NiEu: C, 29.90; H, 2.51; N, 9.69%; found: C, 29.86; H, 2.62; N, 9.67%. IR (KBr, cm⁻¹): 3424 (w), 2948 (w), 2527 (w), 1629 (s), 1560 (w), 1497 (s), 1467 (vs), 1295 (s), 1236 (m), 1168 (w), 1107 (w), 1079 (m), 1029 (w), 987 (w), 952 (w), 861 (w), 813 (w), 785 (w), 740 (m), 683 (w), 625 (w), 604 (w), 580 (w), 542 (w), 494 (w), 439 (w). ESI-MS (*m/z*): 661.01 [M-NO₃]⁺. For **6**: Yield: 0.143 g (65%). Calc. for C₁₈H₁₈N₅O₁₃NiTb: C, 29.62; H, 2.49; N, 9.59%; found: C, 29.58; H, 2.63; N, 9.56%. IR (KBr, cm⁻¹): 3420 (w), 2987 (w), 2846 (w), 1629 (s), 1561 (w), 1501 (s), 1469 (vs), 1316 (w), 1279 (s), 1235 (m), 1167 (m), 1109 (w), 1080 (m), 1027 (w), 990 (w), 956 (w), 861 (w), 811 (w), 784 (w), 740 (m), 685 (w), 626 (w), 582 (w), 543 (w), 495 (w), 438 (w). ESI-MS (*m/z*): 667.98 [M-NO₃]⁺. For **7**: Yield: 0.128 g (58%). Calc. for C₁₈H₁₈N₅O₁₃NiHo: C, 29.38; H, 2.47; N, 9.52%; found: C, 29.34; H, 2.55; N, 9.46%. IR (KBr, cm⁻¹): 3417 (w), 2953 (w), 1628 (s), 1560 (w), 1469 (vs), 1387 (w), 1351 (w), 1295 (vs), 1235 (m), 1170 (m), 1120 (w), 1076 (w), 1028 (w), 964 (w), 858 (w), 813 (w), 785 (w), 740 (m), 685 (w), 615 (w), 584 (w), 543 (w), 493 (w), 472 (w), 441 (w). ESI-MS (*m/z*): 673.98 [M-NO₃]⁺. For **8**: Yield: 0.155 g (70%). Calc. for C₁₈H₁₈N₅O₁₃NiTm: C, 29.22; H, 2.45; N, 9.46%; found: C, 29.17; H, 2.54; N, 9.35%. IR (KBr, cm⁻¹): 3442 (w), 2953 (w), 1628 (s), 1561 (w), 1467 (vs), 1294 (s), 1238 (m), 1197 (w), 1076 (w), 1028 (w), 963 (w), 940 (w), 857 (w), 814 (w), 785 (w), 740 (m), 673 (w), 632 (w), 583 (w), 544 (w), 493 (w), 472 (w), 442 (w). ESI-MS (*m/z*): 677.99 [M-NO₃]⁺.

2.4. Structure determination

Single crystals of [Ni(L)Sm(NO₃)₃]-CH₃COCH₃ (**4**-CH₃COCH₃), [Ni(L)Eu(NO₃)₃]-CH₃COCH₃ (**5**-CH₃COCH₃) or [Ni(L)Tb(NO₃)₃]-

CH₃COCH₃ (**6**-CH₃COCH₃) of suitable dimensions were mounted onto glass fibers for crystallographic analyses, respectively. All the intensity data were collected at 293(2) K on a Bruker SMART CCD diffractometer (Mo-K α radiation, λ = 0.71073 Å) in Φ and ω scan modes. Structure was solved by direct methods followed by difference Fourier syntheses, and refined by full-matrix least-squares techniques against *F*² using SHELXTL [14]. All the non-hydrogen atoms were refined with anisotropic thermal parameters. Absorption corrections were applied using SADABS [15]. All hydrogen atoms were placed in calculated positions and refined isotropically using a riding model. Crystallographic data and refinement parameters for the complex **4**-CH₃COCH₃, **5**-CH₃COCH₃ and **6**-CH₃COCH₃ are presented in Table 1. Selected bond distances and bond angles for the three complexes are given in Table 2.

2.5. Polymerization experiments

L-Lactide was prepared from L-lactic acid as previously reported [16]. The crude product was further purified by re-crystallization three times from dried ethyl acetate, and dried for 24 h in vacuum at 30 °C. Under nitrogen, 1.000 g (6.94 mmol) of the freshly re-crystallized L-lactide monomer and one of the catalysts **1** and **2–8**, in a stipulated molar ratio ([M]/[C]), were charged in an ampoule inside a glove box. The ampoule was put under high vacuum (about 12 Pa) for one hour, after which, the ampoule was sealed under vacuum. The polymerizations were performed in a thermostatically controlled oil bath at 130 or 160 °C for the selected time. Subsequently, the molten reactive polymer mixture was cooled by immersing the sealed ampoule in liquid nitrogen and terminated by introducing absolute MeOH with 5% (w/w) HCl to stop the polymerization. The resulting polylactide (PLA) polymer was dissolved in absolute acetone and precipitate in water. The filtered precipitate was dried under vacuum to constant weight. Molecular weights (*M*_w and *M*_n) and molecular weight distributions (PDI = *M*_w/*M*_n) were determined by gel permeation chromatography (GPC) with polystyrene as standard.

Table 2
Interatomic distances (Å) and bond angles (°) with esds for complexes **4**-CH₃COCH₃, **5**-CH₃COCH₃ and **6**-CH₃COCH₃.

4-CH ₃ COCH ₃		5-CH ₃ COCH ₃		6-CH ₃ COCH ₃	
Ni(1)–N(1)	1.790(20)	Ni(1)–N(1)	1.840(10)	Ni(1)–N(1)	1.852(10)
Ni(1)–N(2)	1.824(17)	Ni(1)–N(2)	1.821(9)	Ni(1)–N(2)	1.835(9)
Ni(1)–O(2)	1.846(12)	Ni(1)–O(2)	1.865(6)	Ni(1)–O(2)	1.849(7)
Ni(1)–O(3)	1.844(12)	Ni(1)–O(3)	1.820(7)	Ni(1)–O(3)	1.850(7)
Sm(1)–O(1)	2.625(13)	Eu(1)–O(1)	2.608(8)	Tb(1)–O(1)	2.552(7)
Sm(1)–O(2)	2.418(12)	Eu(1)–O(2)	2.406(6)	Tb(1)–O(2)	2.351(7)
Sm(1)–O(3)	2.366(12)	Eu(1)–O(3)	2.421(6)	Tb(1)–O(3)	2.403(6)
Sm(1)–O(4)	2.556(14)	Eu(1)–O(4)	2.534(8)	Tb(1)–O(4)	2.566(8)
Sm(1)–O(5)	2.484(14)	Eu(1)–O(5)	2.474(8)	Tb(1)–O(5)	2.481(8)
Sm(1)–O(7)	2.330(30)	Eu(1)–O(7)	2.543(10)	Tb(1)–O(7)	2.494(10)
Sm(1)–O(8)	2.543(16)	Eu(1)–O(8)	2.528(11)	Tb(1)–O(8)	2.478(10)
Sm(1)–O(10)	2.408(18)	Eu(1)–O(10)	2.436(9)	Tb(1)–O(10)	2.462(9)
Sm(1)–O(11)	2.494(12)	Eu(1)–O(11)	2.480(8)	Tb(1)–O(11)	2.429(10)
Sm(1)–O(13)	2.540(30)	Eu(1)–O(13)	2.525(9)	Tb(1)–O(13)	2.485(9)
N(1)–Ni(1)–N(2)	81.1(11)	N(1)–Ni(1)–N(2)	85.3(5)	N(1)–Ni(1)–N(2)	86.2(5)
N(1)–Ni(1)–O(2)	98.4(9)	N(1)–Ni(1)–O(2)	94.2(4)	N(1)–Ni(1)–O(2)	95.6(4)
N(1)–Ni(1)–O(3)	179.7(9)	N(1)–Ni(1)–O(3)	177.3(4)	N(1)–Ni(1)–O(3)	177.5(5)
O(1)–Sm(1)–O(4)	153.9(5)	O(1)–Eu(1)–O(4)	154.5(3)	O(1)–Tb(1)–O(4)	154.3(3)
O(2)–Sm(1)–O(3)	60.7(4)	O(2)–Eu(1)–O(3)	60.8(2)	O(2)–Tb(1)–O(3)	61.6(2)
O(5)–Sm(1)–O(7)	49.6(6)	O(5)–Eu(1)–O(7)	50.5(3)	O(5)–Tb(1)–O(7)	49.7(3)
O(8)–Sm(1)–O(10)	50.5(5)	O(8)–Eu(1)–O(10)	50.5(4)	O(8)–Tb(1)–O(10)	50.8(4)
O(11)–Sm(1)–O(13)	50.2(7)	O(11)–Eu(1)–O(13)	50.4(3)	O(11)–Tb(1)–O(13)	51.8(3)

3. Results and discussion

3.1. Synthesis and characterization

As shown in Scheme 2, reaction of an equimolar amount of **H₂L** and Ni(OAc)₂·4H₂O in absolute EtOH afforded complex **1** in good yield. Further reaction of **1** with Ln(NO₃)₃·6H₂O (Ln = Ce, Nd, Sm, Eu, Tb, Ho or Tm) in 1:1 molar ratio in EtOH-DMF resulted in the formation of complex **2–8**, respectively. The IR spectra of **1** and **2–8** show the characteristic absorptions of the ν(C=N) vibration at 1642 cm⁻¹ for **1** and 1628–1630 cm⁻¹ for **2–8**, are slightly blue or red shifted by ca. 10 or 2–4 cm⁻¹ relative to those of the free Salen-type ligand **H₂L** (1632 cm⁻¹ for **H₂L**) upon coordination of metal ions [17], respectively. For **2–8**, two strong absorption bands at 1466–1470 and 1276–1296 cm⁻¹ attributed to ν(NO₃⁻) [18]. Thermogravimetric analysis (TGA) in the range 25–600 °C showed that the framework of **1** or **2–8** decomposes at temperature over 298 °C where an abrupt weight loss was observed, followed by a final weight loss in the 305 (**1**) or 313–342 (**2–8**) to 600 °C range. As to the solution behavior of complexes **1–8**, the ESI-MS spectra exhibit one peak at *m/z* 386.04 and 649.17–677.99, respectively, corresponding to the major species [NiL-H]⁺ and [NiLn(NO₃)₂]⁺, and indicating that the respective discrete monometallic or bimetallic molecule exists in dilute CHCl₃ solution. For the selected complexes **1** and **4**, further from the UV–visible absorption spectra of the free ligand and the two complexes examined in dilute CHCl₃ solution, as shown in Fig. 1, the free ligand **H₂L** exhibits absorption bands at 220, 264, 296, 334 and 429 nm, which could be assigned to the ligand-centered π → π* transitions, while for the two complexes **1** and **4**, the lower energy bands are significantly blue-shifted upon coordination to metal ions (243, 338 and 400 nm for **1**; 241, 334 and 385 nm for **4**).

3.2. Structures

For complex **1**, the room temperature ¹H NMR spectrum in CDCl₃ exhibits one set of the proton resonances of the **L²⁻** ligand, significantly red-shifted in relative to those of the free ligand, which shows a typical monometallic structure of [NiL] in solution. The X-ray crystal structure analysis of the three complexes [NiLn(NO₃)₃]:CH₃COCH₃ (Ln = Sm, **4**-CH₃COCH₃; Ln = Eu, **5**-CH₃COCH₃; Ln = Tb, **6**-CH₃COCH₃) unambiguously revealed the

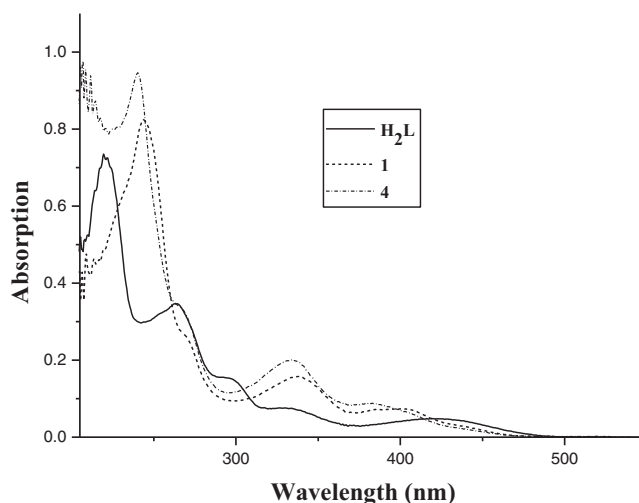
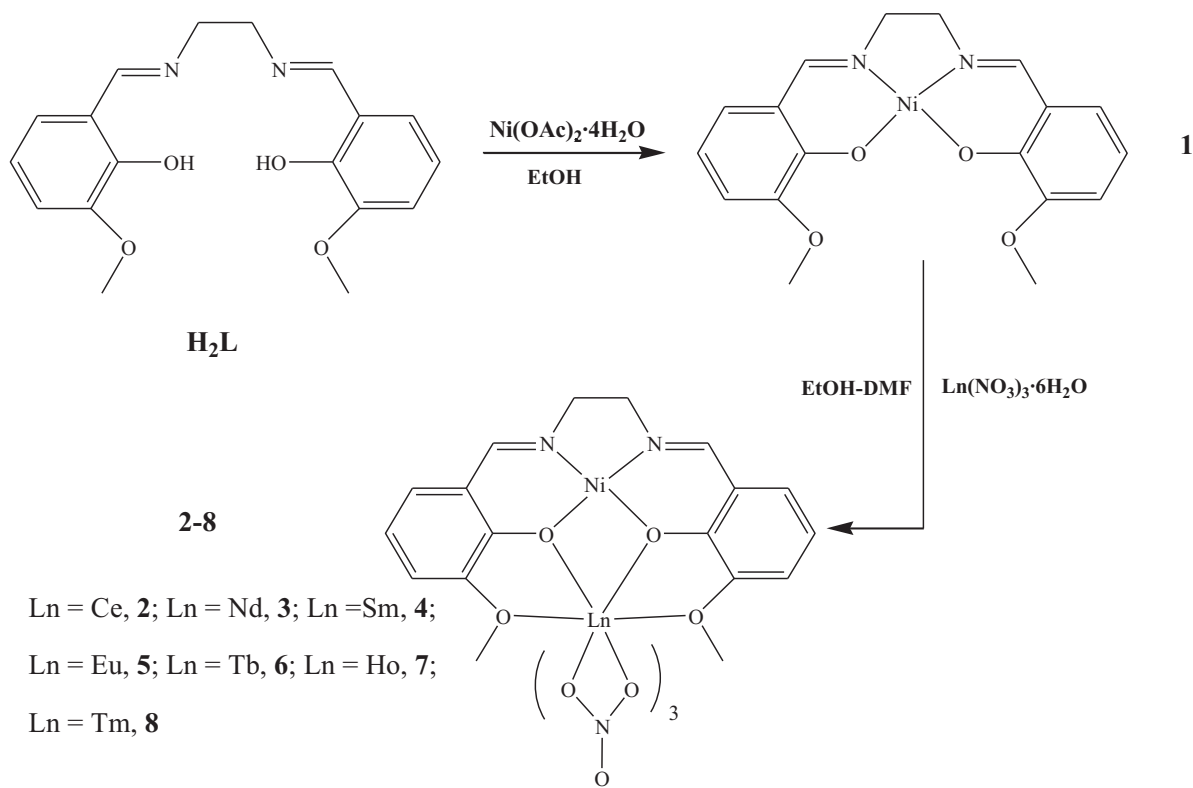


Fig. 1. UV–visible absorption spectra of **H₂L**, **1** and **4** in CHCl₃ at 2 × 10⁻⁵ M at room temperature.

isostructural bimetallic Ni–Ln structure, as depicted in Figs. 2–4. Each of neutral host structures revealed that the relatively soft Ni²⁺ ion is located in the inner N₂O₂ core, the relatively hard Ln³⁺ ion in the outer O₂O₂ cavity of the Schiff base **L²⁻** ligand. The Ni²⁺ ion lies in a four-coordinate environment and adopts a slightly distorted square-planar geometry, with two sets of unequal Ni–N(imino) (1.790(20)–1.824(17) Å for **4**, 1.821(9)–1.840(10) Å for **5** and 1.835(9)–1.852(10) Å for **6**) and Ni–O (phenolic) (1.844(12)–1.846(12) Å for **4**, 1.820(7)–1.865(6) Å for **5** and 1.849(7)–1.850(7) Å for **6**) bond lengths and N–Ni–O bond angles (98.4(9)–98.6(10)° and 178.8(7)–179.7(9)° for **4**, 94.2(4)–97.4(4)° and 177.3(4)–179.5(4)° for **5** and 95.6(4)–95.9(4)° and 177.7(5)–177.9(4)° for **6**). Each of the Ln³⁺ ions in the three complexes is ten coordinated and bound by four O atoms from the Schiff base **L²⁻** ligand, and six from three bidentate NO₃⁻ groups. The Ln–O bond lengths depend on the nature of the oxygen atoms: they vary from 2.330(30) to 2.625(13) Å for **4** (2.406(6) to 2.608(8) Å for **5** and 2.351(7) to 2.566(8) Å for **6**), and the bond lengths from phenoxo oxygen atoms are shorter than those from oxygen atoms of bidentate NO₃⁻ anions. It is worth noting that in the three



Scheme 2. Reaction scheme for the syntheses of complexes **1** and **2-8**.

bimetallic complexes, the coordination of the different rare ions leads to the difference of coordination geometries of Ni^{2+} ions, in agreement with that of magnetic Cu–Ln [19] or luminescent Zn–Ln [20] Salen-type Schiff-base complexes. Furthermore, this point also endows that the change of the intramolecular Ni...Ln (Ln = Sm, **4**; Ln = Eu, **5**; Ln = Tb, **6**) separations (2.432(2) Å for **4**; 2.437(2) Å for **5**; 2.411(2) Å for **6**) does not strictly keep to the order of Lanthanide Contraction [21], which should be relative to the catalysis. For the three complexes, the solvates are not bound to the framework and they exhibit no observed interactions with the host structure.

3.3. The polymerization studies of L-lactide

The ROP of L-lactide using the two kinds of complexes **1** or **2-8** as catalysts in a stipulated molar ratio of $[\text{M}]/[\text{C}]$ were carried out at 130 or 160 °C for the selected time under solvent-free melt conditions. Under these conditions (entries 3–20), the reaction mixture would form a monomer melt in which the polymerization would occur, and the results were summed in Table 3. For complex **1**, at the polymerization temperature of 130 °C, the cat-

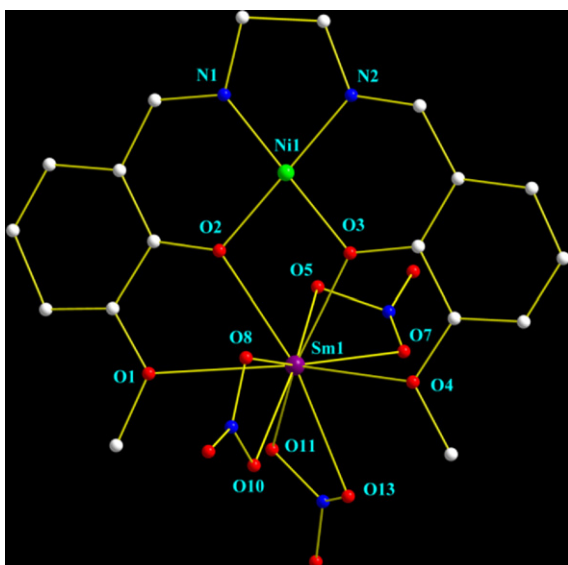


Fig. 2. Structure scheme of complex **4**- CH_3COCH_3 , hydrogen atoms and solvates are omitted for clarity.

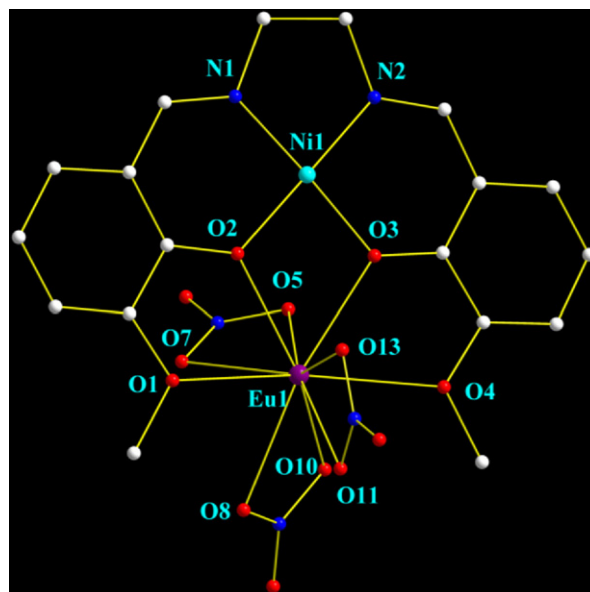


Fig. 3. Structure scheme of complex **5**- CH_3COCH_3 , hydrogen atoms and solvates are omitted for clarity.

Table 3
Catalytic data in the bulk polymerization of L-lactide.

Entry	Compound	Time (h)	T (°C)	M/[C] ^a ratio	Activity (g mol ⁻¹ h ⁻¹)	M _n ^b (10 ³)	M _w ^c (10 ³)	PDI ^d
1	–	24	130		0	–	–	–
2	H ₂ L	24	130	1000/1	0	–	–	–
3	1	12	130	1000/1	240.5	10.383	12.228	1.178
4	1	24	130	1000/1	392.2	22.702	26.635	1.173
5	1	36	130	1000/1	398.4	22.596	31.385	1.389
6	1	24	160	1000/1	402.7	20.829	31.994	1.536
7	1	24	130	500/1	401.0	22.071	26.662	1.208
8	1	24	130	2000/1	110.7	25.494	31.664	1.242
9	2	12	160	1000/1	393.7	30.154	34.104	1.131
10	3	12	160	1000/1	351.7	30.702	34.998	1.140
11	4	12	130	1000/1	289.3	17.381	20.235	1.164
12	4	24	130	1000/1	375.3	26.940	30.146	1.119
13	4	36	130	1000/1	384.6	26.705	30.791	1.153
14	4	12	160	1000/1	401.8	30.632	34.431	1.124
15	4	24	130	500/1	419.4	22.389	29.531	1.319
16	4	24	130	2000/1	180.8	25.883	34.425	1.330
17	5	12	160	1000/1	415.6	28.961	34.463	1.190
18	6	12	160	1000/1	376.5	31.555	35.815	1.135
19	7	12	160	1000/1	308.2	30.035	34.570	1.151
20	8	12	160	1000/1	415.9	30.659	35.657	1.163

^a [M]/[C] ratio is the molar ratio of L-lactide monomer and catalyst.

^b M_n is the relative number-average molecular weight.

^c M_w is the relative weight-average molecular weight.

^d PDI = M_w/M_n.

alytic activities increased with the increase of reaction times, and the well-controlled polymerization was observed from the narrow molecular weight distributions (PDI = 1.173–1.389). The highest M_n (M_n = 22,702) and the smallest PDI value (PDI = 1.173) of the products were achieved by polymerization for 24 h and the molecular weight distribution (PDI = 1.389) broadened with prolonging polymerization time (36 h), which should be attributed to the thermal depolymerization [22]. Similar to the polymerization with the prolonged time, the result of ROP of L-lactide performed at temperatures ranging from 130 to 160 °C for 24 h (entry 6) showed that with increasing temperature, the catalytic activity increased, however, the molecular weight decreased and the molecular weight distribution broadened. This may also be ascribed to the thermal depolymerization and the acceleration of transesterification as the polymerization temperature increases [23]. When the [M]/[C] ratio was lower than [1000]/[1], little difference was found in spite

of the increase of the polymer yields and the catalytic activities. The molecular weights (M_n and M_w) of the polymeric products were also affected by the [M]/[C] ratio: The maximum of molecular weight (M_n = 25,494 or M_w = 31,664) was achieved at an [M]/[C] ratio of 2000/[1], which showed that the lower catalyst concentration could be helpful for the growth of the polymeric products; While a lower catalyst concentration will produce less initiation sites, thus leading to the lower catalytic activities [24]. It is worth noting that in the selected range (500–2000/1) of [M]/[C] ratios, the Ni²⁺ catalyst **1** could afford the PLAs with narrow molecular weight distributions (M_w/M_n = 1.173–1.242), while the blank experiment (entry 1) or the presence of free ligand (entry 2) showed that no polymeric products were obtained, both further demonstrates that the presence of single site active species (Ni²⁺) in **1** endows the controllable polymerization process [25]. It is worth comparing that the catalytic behaviors between the catalyst **1** with other known catalysts based on Salen-type Schiff-base ligands for the ring-opening polymerization of L-lactide in solutions or under the solvent-free melt conditions. In contrast to the solution polymerization, transition metal complexes [11] of Salen-type chiral or achiral Schiff-base ligands, necessarily with the assistance of the characteristic initiators in the possible coordination-insertion mechanism, can be efficient catalysts with higher catalytic performances for the ring-opening polymerization of L-lactide on the condition of low temperatures and short times, while the catalyst **1** could also efficiently catalyze the bulk solvent-free melt ring-opening polymerization (ROP) of L-lactide with moderate catalytic activities (as shown in Table 3), as founded for the Fe²⁺ or Mn³⁺ Salen-type Schiff-base complexes [12]. Especially the further investigation for the catalysts without those initiators shows that lower temperature (130 °C) and longer reaction time (24 or 36 h) or higher temperature (>160 °C) and shorter reaction time (<4 h) are feasible to obtain the PLA product in the controllable mode.

For the selected complex **4**, on the varied reaction conditions, the better controllable polymerization (entries 11–16) of L-lactide was observed, which was also summed in Table 3. It is significant on the correlation on the molecular structure of complex **4** versus the catalytic behavior. The further coordination of Sm(NO₃)₃ in complex **4** endowed the slight distortion of square-planar geometry and the increase of Lewis acidity of the four-coordinate Ni²⁺ ion. On the condition of short reaction time (12 h) or high catalyst concentration

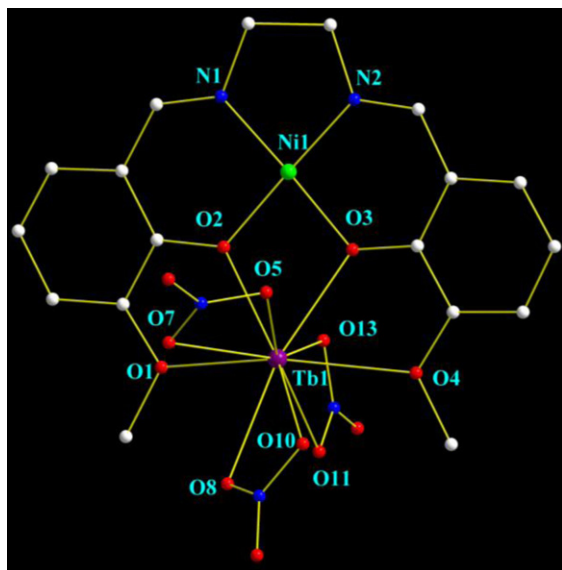


Fig. 4. Structure scheme of complex **6**-CH₃COCH₃, hydrogen atoms and solvates are omitted for clarity.

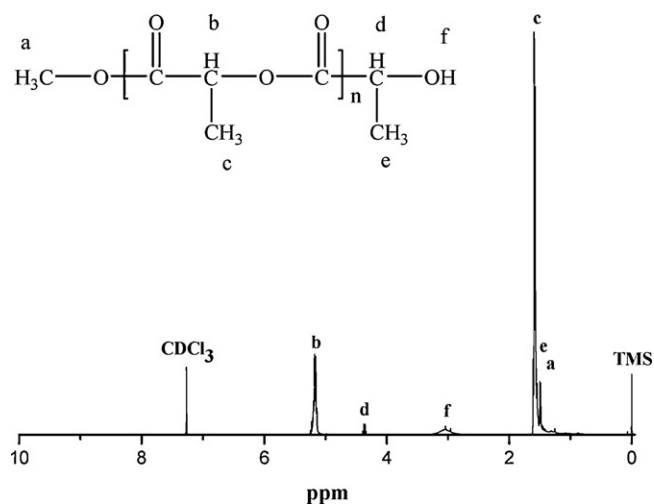


Fig. 5. ^1H NMR spectrum in CDCl_3 of PLA prepared by complex 1 or 4 from ROP of L-lactide.

($[\text{M}]/[\text{C}] = 500/[\text{I}]$) at 130°C , complex **4** showed higher catalytic activity than that of complex **1**, respectively. When the reaction time was prolonged or the catalyst concentration was increased, an obvious decrease of catalytic activities was observed, which shows that the steric effect from the coordination of $\text{Sm}(\text{NO}_3)_3$ in complex **4** should prevent the coordination with the active species for L-lactide monomers. Actually, due to the existence of nitrates around the Sm^{3+} ions in complex **4**, in agreement with its solution behavior, the second metal center (Sm^{3+}) was inactive to the ROP of L-lactide. However, for the obtained polymeric products by complex **4**, a significant increase in molecular weights (M_w or M_n) was observed, which suggests that the steric effect from the coordinated $\text{Sm}(\text{NO}_3)_3$ in complex **4** is in favor of the growth of polymer chains in further insertion for L-lactide monomers, even at 160°C for 12 h or 130°C for 36 h.

It is of special interest to compare the inherent relationship between the molecular structures and the catalytic behaviors for the seven isostructural complexes **2–8** with different rare ions. As a whole, with the further involvement of rare ions, higher molecular weights ($M_n = 28,961\text{--}31,555$ and $M_w = 34,104\text{--}35,815$) and better controllable polymerizations ($\text{PDI} = 1.124\text{--}1.190$, entries 9, 10, 12 and 17–20, Table 3) was obtained relative to that of complex **1**, even on the condition of 160°C for 12 h. It is especially worth noting that, for the three complexes **4–6**, the catalytic activities are in the order of **5** > **4** > **6**, which shows that the trend is relative to the intramolecular $\text{Ni}\cdots\text{Ln}$ separations (Section 3.2) while no sequence of Lanthanide Contraction [21].

Thermogravimetric analysis (TGA) in the range of $25\text{--}600^\circ\text{C}$ showed that these perspective polymeric products (entry 4 and entry 10) decomposed at temperature over 240°C (243°C by **1** and 261°C by **4**), where an abrupt weight loss was observed, followed by a final weight loss in the $375\text{--}600^\circ\text{C}$ range. One of the identical FT-IR spectra shows the characteristic absorption bands of PLA: the weak and broad peak at 3442 cm^{-1} assigned to the $-\text{OH}$ stretching vibration; the peaks at 2999, 2950 and 2875 cm^{-1} assigned to the asymmetric $-\text{CH}_3$, symmetric $-\text{CH}_3$ and weak $-\text{CH}$ stretching vibrations, respectively; a very strong peak at 1758 cm^{-1} assigned to the $-\text{C}=\text{O}$ stretching vibration; and peaks at $1192\text{--}1245\text{ cm}^{-1}$, $1090\text{--}1132\text{ cm}^{-1}$ and 756 cm^{-1} attributed to the asymmetric $-\text{C}-\text{O}-\text{C}-$ vibration, the symmetric $-\text{C}-\text{O}-\text{C}-$ vibration and the $-\text{C}=\text{O}$ bending vibration, respectively. One of the identical ^1H NMR spectra of the polymers (as shown in Fig. 5) showed a doublet at 1.59 ppm for the methyl (^aH) and a multiplet at 5.18 ppm for the methine (^bH) of main chain of PLA, indicating no inversion of the configuration of asymmetric carbon atoms of the monomer under

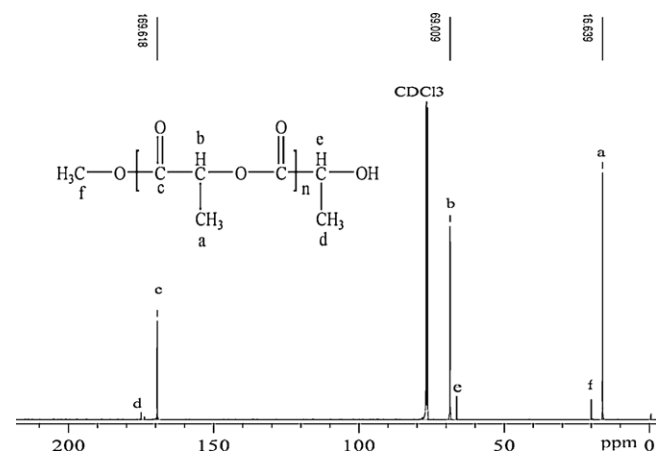


Fig. 6. ^{13}C NMR spectrum in CDCl_3 of PLA prepared by complex 1 or 4 from ROP of L-lactide.

the reaction conditions. The additional signals appearing at 1.49, 3.04 and 4.36 ppm should be assigned to the methyl, the hydroxyl end group and the methine of PLA, respectively. Fig. 6 shows the ^{13}C NMR spectrum of the selected PLA, in which the peaks at 16.64, 69.00 and 169.62 ppm were observed and should be assigned to methyl carbon, methane carbon and ester carbon, respectively, in agreement with the corresponding carbon atoms of the chemical structure, and the PLA is isotactic in nature [26]. It is worth noting that the systems **1–8** are active for the bulk ROP of L-lactide in the absence of normal initiators (alkoxide, amide or carboxylate), and the end groups of PLA are not from the catalysts, as also checked by the ^1H NMR spectroscopy (as shown in Fig. 5) and the MALDI-TOF (as shown in Supporting information) results of the oligomer sample, but probably from the replacement of methyl groups when terminating the polymerization with methanol containing 5% HCl. Thus, the initiation may occur through the metal-alkoxide bond of the catalysts, and through the stable and selective acyl-oxygen bond cleavage of the monomer, the ring-opening polymerization also proceeds via the typical “coordination–insertion” mechanism [1(a)].

4. Conclusion

In conclusion, the monometallic Ni^{2+} complex **1** and the bimetallic $\text{Ni}^{2+}\text{--}\text{Ln}^{3+}$ complexes **2–8** were shown to could efficiently catalyze the bulk solvent-free melt ring-opening polymerization (ROP) of L-lactide with moderate molecular weights and narrow molecular weight distributions. The correlation of molecular structure versus catalytic activity showed that the different catalytic behaviors resulted from the different active species, especially, the involvement of rare ions effectively passivated the catalytic behaviors on the ROP of L-lactide, being in favor of the increase of polymeric molecular weights (M_w or M_n) and the polymerization controllability. With these in mind, the design of higher active and multiple active species catalysts is now under way.

5. Supplementary material

The MALDI-TOF result analysis was founded in the Supporting information. Crystallographic data for the structural analyses have been deposited with the Cambridge Crystallographic Data Center, CCDC reference numbers for **4**: CH_3COCH_3 , **5**: CH_3COCH_3 and **6**: CH_3COCH_3 are 776507–776509, respectively. Copies of this information may be obtained free of charge from The Director, CCDC, 12 Union Road, Cambridge, CB2 1EZ UK (Fax: +44 1223 336033; email: deposit@ccdc.cam.ac.uk or www: <http://www.ccdc.cam.ac.uk>).

Acknowledgements

This work was supported by the National Natural Science Foundation of China (20871098), the State Key Laboratory of Structural Chemistry (20100014), the Provincial Key Item of Shaanxi, Graduate Innovation and Creativity Funds (08YZZ48), Graduate Cross-discipline Funds (09YJC23) and Bachelor Graduate Innovation and Creativity Funds of Northwest University in PR China.

Appendix A. Supplementary data

Supplementary data associated with this article can be found, in the online version, at [doi:10.1016/j.molcata.2011.01.009](https://doi.org/10.1016/j.molcata.2011.01.009).

References

- [1] (a) O. Dechy-Cabaret, B. Martin-Vaca, D. Bourissou, *Chem. Rev.* 104 (2004) 6147; (b) M. Vert, *Biomacromolecules* 6 (2005) 538.
- [2] (a) J.C. Wu, T.L. Yu, C.T. Chen, C.C. Lin, *Coord. Chem. Rev.* 250 (2006) 602; (b) N.E. Kimura, W. Jeong, R.M. Waymouth, R.C. Pratt, B.G.G. Lohmeijer, J.L. Hedrick, *Chem. Rev.* 107 (2007) 5813; (c) R.H. Platel, L.M. Hodgson, C.K. Williams, *Polym. Rev.* 48 (2008) 11.
- [3] M.J. Stanford, A.P. Dove, *Chem. Soc. Rev.* 39 (2010) 486.
- [4] A.C. Albertsson, I.K. Varma, *Biomacromolecules* 4 (2003) 1466.
- [5] J.H. Khan, F. Schue, G.A. George, *Polym. Int.* 58 (2009) 296.
- [6] (a) X.Y. Wang, K.R. Liao, D.P. Quan, Q. Wu, *Macromolecules* 38 (2005) 4611; (b) A.J. Chmura, C.J. Chuck, M.G. Davidson, M.D. Jones, M.D. Lunn, S.D. Bull, M.F. Mahan, *Angew. Chem. Int. Ed.* 46 (2007) 2280.
- [7] (a) M.K. Samantaray, V. Katiyar, D. Roy, K. Pang, H. Nanavati, R. Stephen, R.B. Sunoj, P. Ghosh, *Eur. J. Inorg. Chem.* 15 (2006) 2975; (b) L. Ray, V. Katiyar, M.J. Raihan, H. Nanavati, M.M. Shaikh, P. Ghosh, *Eur. J. Inorg. Chem.* 15 (2006) 3724; (c) L. Ray, V. Katiyar, S. Barman, M.J. Raihan, H. Nanavati, M.M. Shaikh, P. Ghosh, *J. Organomet. Chem.* 692 (2007) 4259; (d) A. John, V. Katiyar, K. Pang, M.M. Shaikh, H. Nanavati, P. Ghosh, *Polyhedron* 26 (2007) 4033; (e) A.D. Schwarz, A.L. Thompson, P. Mountford, *Inorg. Chem.* 48 (2009) 10442;
- (f) J. Börner, U. Flörke, T. Glöge, T. Bannenberg, M. Tamm, M.D. Jones, A. Döring, D. Kuckling, S. Herres-Pawlis, *J. Mol. Catal. A: Chem.* 316 (2010) 139.
- [8] (a) E.L. Marshall, V.C. Gibson, H.S. Rzepa, *J. Am. Chem. Soc.* 127 (2005) 6048; (b) M.H. Chisholm, N.J. Patmore, Z.P. Zhou, *Chem. Commun.* 1 (2005) 127.
- [9] (a) N.S. Venkataramanan, S. Natarajan, G. Kuppuraj, S. Rajagopai, *Coord. Chem. Rev.* 249 (2005) 1249; (b) C. Baleizao, H. Garcia, *Chem. Rev.* 106 (2006) 3987; (c) D.J. Darensbourg, *Chem. Rev.* 107 (2007) 2388; (d) K.C. Gupta, A.K. Sutar, *Coord. Chem. Rev.* 252 (2008) 1420.
- [10] D.A. Atwood, M.J. Harvey, *Chem. Rev.* 101 (2001) 37.
- [11] (a) P.A. Cameron, D. Jhurry, V.C. Gibson, A.J.P. White, D.J. Williams, S. Williams, *Macromol. Rapid Commun.* 20 (1999) 616; (b) J.C. Wu, B.H. Huang, M.L. Hsueh, S.L. Lai, C.C. Lin, *Polymer* 46 (2005) 9784; (c) P. Hornmiron, E.L. Marshall, V.C. Gibson, R.I. Pugh, A.J.P. White, *Proc. Natl. Acad. Sci. U.S.A.* 103 (2006) 15343; (d) R.J.C. Atkinson, K. Gerry, V.C. Gibson, N.J. Long, E.L. Marshall, L.J. West, *Organometallics* 26 (2007) 316; (e) M.H. Chisholm, J.C. Gallucci, K.T. Quisenberry, Z.P. Zhou, *Inorg. Chem.* 47 (2008) 2613.
- [12] B.B. Idage, S.B. Idage, A.S. Kasegaonkar, R.V. Jadhav, *Mater. Sci. Eng. B* 168 (2010) 193.
- [13] X.Q. Lü, W.Y. Bi, W.L. Chai, J.R. Song, J.X. Meng, W.Y. Wong, W.K. Wong, R.A. Richard, *New J. Chem.* 32 (2008) 127.
- [14] G.M. Sheldrick, *SHELXS-97: Program for Crystal Structure Refinement*, 1997 (Göttingen, Germany).
- [15] G.M. Sheldrick, *SADABS*, University of Göttingen, 1996.
- [16] K.S. Anderson, K.M. Schreck, M.A. Hillmyer, *Polym. Rev.* 48 (2008) 85.
- [17] X.Q. Lü, W.Y. Wong, W.K. Wong, *Eur. J. Inorg. Chem.* 4 (2008) 523.
- [18] K. Nakamoto, *Infrared and Raman Spectra of Inorganic and Coordination Compounds*, 4th ed., Wiley, New York, 1986 (Sect. II. 8).
- [19] W.B. Sun, P.F. Yan, G.M. Li, J.W. Zhang, H. Xu, *Inorg. Chim. Acta* 362 (2009) 1761.
- [20] W.Y. Bi, X.Q. Lü, W.L. Chai, W.J. Jin, J.R. Song, W.K. Wong, *Inorg. Chem. Commun.* 11 (2008) 1316.
- [21] B.G. Wybourne, *Spectroscopic Properties of Rare Earths*, John-Wiley & Sons Inc., New York/London/Sydney, 1965.
- [22] S.H. Hyon, K. Jamshidi, Y. Ikada, *Biomaterials* 18 (1997) 1503.
- [23] D. Mecerreyes, R. Jerome, *Macromol. Chem. Phys.* 200 (1999) 2581.
- [24] J.P. Puaux, I. Banu, I. Nagy, G. Bozga, *Macromol. Symp.* 259 (2007) 318.
- [25] M.H. Chisholm, Z.P. Zhou, *J. Mater. Chem.* 14 (2004) 3081.
- [26] (a) I. Peckermann, A. Kapelski, T.P. Spaniol, J. Okuda, *Inorg. Chem.* 48 (2009) 5526; (b) X.B. Pan, A. Liu, X.H. Yang, J.C. Wu, N. Tang, *Inorg. Chem. Commun.* 13 (2010) 376.